Asian Journal of Atmospheric Environment
Vol. 9-1, pp. 78-85, March 2015
doi: http://dx.doi.org/10.5572/ajae.2015.9.1.078

ISSN(Online) 2287-1160
ISSN(Print) 1976-6912

Characterization of Particulate Emissions from Biodiesel using High Resolution Time of Flight Aerosol Mass Spectrometer

Yongjoo Choi, Jinsoo Choi[1)], Taehyun Park, Seokwon Kang and Taehyoung Lee*

Department of Environmental Science, Hankuk University of Foreign Studies, Yongin, Korea
[1)]Climate & Air Quality Research Department, National Institute of Environmental Research, Incheon, Korea

*Corresponding author. Tel: +82-31-330-4039, E-mail: thlee@hufs.ac.kr

ABSTRACT

In the past several decades, biofuels have emerged as candidates to help mitigate the issues of global warming, fossil fuel depletion and, in some cases, atmospheric pollution. To date, the only biofuels that have achieved any significant penetration in the global transportation sector are ethanol and biodiesel. The global consumption of biodiesel was rapidly increased from 2005. The goal of this study was to examine the chemical composition on particulate pollutant emissions from a diesel engine operating on several different biodiesels. Tests were performed on non-road diesel engine. Experiments were performed on 5 different fuel blends at 2 different engine loading conditions (50% and 75%). 5 different fuel blends were ultra-low sulfur diesel (ULSD, 100%), soy biodiesel (Blend 20% and Blend 100%) and canola biodiesel (Blend 20% and Blend 100%). The chemical properties of particulate pollutants were characterized using an Aerodyne High Resolution Time of Flight Aerosol Mass Spectrometer (HR-ToF-AMS). Organic matter and nitrate were generally the most abundant aerosol components and exhibited maximum concentration of 1207 $\mu g/m^3$ and 30 $\mu g/m^3$, respectively. On average, the oxidized fragment families ($C_xH_yO_1^+$, and $C_xH_yO_z^+$) account for ~13% of the three family sum, while ~87% comes from the $C_xH_y^+$ family. The two peaks of $C_2H_3O_2$ (*m/z* 59.01) and C_3H_7O (*m/z* 59.04) located at approximately *m/z* 59 could be used to identify atmospheric particulate matter directly to biodiesel exhaust, as distinguished from that created by petroleum diesel in the AMS data.

Key words: Biodiesel, Aerosol mass spectrometer, Particulate emission, Aerosol oxidation, Marker

1. INTRODUCTION

The global consumption of natural resources (e.g. fossil fuels) is directly proportional to the global population and the gross domestic product per capita. With today's sustained levels of population growth, along with unprecedented economic growth among developing economies, the depletion of fossil fuels promises to be a civilization-scale challenge that will be faced by the human race at some point in the not too distant future. In fact, current estimates predict that the world oil supply could be depleted within the next fifty years, with some models predicting a much sooner date (Appenzeller, 2004). In the transportation sector, 97% of all energy consumption is derived from the combustion of liquid, petroleum-based fossil fuels (Chapman, 2007). Liquid biofuels, which are derived from renewable resources such as plants and animal byproducts, have the potential to reduce the rate of fossil fuel depletion. Our need to find an alternative to petroleum is not only driven by diminishing supply and increasing demand, but also with the intention of reducing the environmental effects caused by combustion of petroleum products. The pollutants produced by the transportation sector contribute to smog, ground level ozone and a variety of negative health effects. The 5th Report by the Intergovernmental Panel on Climate Change (IPCC) concluded that global warming is occurring and that CO_2 emissions from the combustion of fossil fuels are largely responsible.

In the past several decades, biofuels have emerged as candidates to help mitigate the issues of global warming, fossil fuel depletion and, in some cases, atmospheric pollution. To date, the only biofuels that have achieved any significant penetration in the global transportation sector are ethanol and biodiesel. However, ethanol, made through the fermentation of starch, and biodiesel, the product of transesterifing triglycerides, are not the only fuels that can be created

from renewable sources. The same technology used to convert crude petroleum into jet fuel, diesel, and gasoline can be used on biomass or plant oil (U.S. Department of Energy, 2009). The thermal or catalytic cracking process can be used on triglycerides to remove oxygen and break down the hydrocarbon chains to the lengths required to make renewable diesel, renewable jet fuel, and renewable alcohols. The production of biodiesel in the U.S. in 2008 was roughly 0.7 billion gallons, which is well below the production capacity in the U.S. of 2.7 billion gallons. However, the production of the biodiesel was rapidly increased from 2005 (National Biodiesel Board, 2009) and also the global consumption of biodiesel was continually increased.

Biodiesel from vegetable oil is considered nearly carbon neutral, as the plants take in nearly the same amount of CO_2 during growth as that which is expelled during the combustion of the oil they produce (Sheehan *et al*., 1998). When biodiesel is burned in a diesel engine, many combustion products, such as carbon monoxide (CO) and total hydrocarbons (THC), are reduced (Demirbas, 2007; USEPA, 2002). Feedstock for biodiesel, such as soybeans and canola, can be grown domestically so increasing our use of biodiesel would help reduce our dependence on foreign oil and create domestic jobs. While most of the emissions are improved with biodiesel, nitrogen oxides (NO_x) have generally been shown to increase with biodiesel. NO_x are a regulated emission in the vehicles because they contribute to photochemical smog, acid rain and ground level ozone. Many authors have indicated that the usage of biodiesel decreases the emissions of HC, CO and PM and the improvements are mainly due to the higher oxygen content of the fuels compared to diesel fuel (Gordon *et al*., 2014; Di *et al*., 2009; Karavalakis *et al*., 2009; Lapuerta *et al*., 2008; Mayer *et al*., 2005). A reduction in the organic aerosol emissions was also observed with 10% biodiesel blend and with 30% biodiesel blend as reduced by 22% and 21% than Diesel (Chirico *et al*., 2014). In case of PAH, its molecular weight distribution is not significantly affected by the fuel composition, and that sulfates are reduced by increased biodiesel content. Octanedioic acid (a carbonyl species) is increased with increased biodiesel concentration (Dutcher *et al*., 2011). However, recent studies revealed an increase in particle number emission in the nucleation mode when biodiesel blends were used but the very low sulfur content of biodiesel fuels can also be an explanation for the decrease in nanoparticle concentrations (Lapuerta *et al*., 2008; Aakko *et al*., 2002; Kittelson *et al*., 1998).

In general, most of studies have focused on the particle size distribution and/or number concentration from biodiesel (Young *et al*., 2012; Zhu *et al*., 2010; Heikkilä *et al*., 2009; De Filippo *et al*., 2008; Kittelson *et al*., 2006; Bagley *et al*., 1998). The chemical properties of particulate pollutants from biodiesel could have adverse health consequences since smaller particles can be inhaled deeper into the lungs (Kittelson, 1998) and it is the organic matter on the particles that has been linked to many of the health effects that have been associated with diesel exhaust such as cancer, respiratory ailments and heart disease (Gaffney and Marley, 2009). Despite all the potential benefits of biodiesel, significant improvements must be made if widespread use is ever to be achieved. In this study, we were to examine the general chemical composition including the status of oxidation on particulate pollutant emissions from a diesel engine operating on biodiesel and obtained mass spectra from regular petroleum-based diesel and two types of biodiesel under controlled conditions.

2. INSTRUMENTATION

The Aerodyne High-Resolution Time-of-Flight Aerosol Mass Spectrometer (Hereafter AMS) contains a high-resolution time-of-flight mass spectrometer that can characterize the elemental composition of the organic carbon content of the particulate matter. The specific chemical breakdown of the exhaust products provides more insight on the health and environmental effects due to the combustion of different fuels. The exhaust sample from the dilution tunnel passes through a $PM_{2.5}$ cyclone (3 LPM, URG-2000-30ED) and a critical orifice, restricting the flow to 0.1 LPM, before entering the AMS. Perma Pure dryers (MD-110-24) were used to control sample humidity ($<40\%$ RH), reducing uncertainties due to bounce-related changes in collection efficiency and reduced particle transmission through the aerodynamic lens. The exhaust air enters the AMS through a critical orifice (1 μm size cut) into an aerodynamic lens, creating a narrow particle beam. The particles are accelerated in the supersonic expansion of gas molecules into vacuum at the end of the aerodynamic lens. Particle packets are selected by chopper for separation as a function of size in the PToF region. Non-refractory particles are vaporized, and the fragments are then ionized (E) and sent through the ToF-MS region utilizing either the V flight path. The ion flight time to the detector corresponds to a specific mass-to-charge ratio, *m/z*. The operation of the Aerodyne HR-ToF-AMS has been described in detail elsewhere (e.g. DeCarlo *et al*., 2006; Drewnick *et al*., 2005; Jimenez *et*

al., 2003; Jayne *et al*., 2000).

The AMS was calibrated for nitrate ionization efficiency (IE) through introduction of 350 nm ammonium nitrate particles (typical value IE_{NO3}~1.53e-07 ions/molecule). Relative ionization efficiencies (RIEs) for other aerosol types were taken from published values (note that RIE of NH_4 of 4.5 was measured during nitrate ionization efficiency). The timeline of Composition-Dependent collection efficiency (CDCE) was calculated based on AMS chemical composition and experiments under low humidity conditions and was used for the AMS quantitative analysis (Middlebrook, 2011). The default value of 370 ppm of CO_2 was used to correct our data for any potential interference with the signal at *m*/*z* 44 (CO_2^+) in the AMS (Note that AMS sampled particulate pollutants from 40 : 1 dilution chamber and the concentration of CO_2 in chamber was slightly higher than typical ambient mixing ratio of ~370 ppm. We found that the interference by the doubled CO_2 concentration is positively biased less than 0.2% of our reported organic concentration). The AMS samples particles roughly 10^6 times more efficiently than the gas-phase.

Primary data processing will be started with integrating the results of all calibrations, logged events, and background data (air beam, etc.) with raw data to produce the initial unit mass resolution (UMR) data; *m*/*z* calibrations, baseline signal, and single ion signal areas are also verified. Primary data processing uses the SQUIRREL program (v1.56) in Igor Pro 6 (Wavemetrics, Lake Oswego, OR), and products include species timelines, average diurnal variations, and the spectra that comprise the PMF input. The secondary data processing addresses error in high-resolution peak shape and assigns fragments to species families using the Igor-based PIKA program (v1.15). High-resolution mass spectrometry allows discernment between fragments that share the same UMR bin as described earlier.

Tests were performed on non-road diesel engine without diesel particulate filter (DPF) using 5 different fuel blends (ultra-low sulfur diesel (ULSD, 100%), soy biodiesel (Blend 20% and Blend 100%) and canola biodiesel (Blend 20% and Blend 100%)) at 2 different engine loading conditions (50% and 75%). In order to better simulate tailpipe exhaust and allow time for the complex agglomerates of carbon particles to grow into particulate matter as they naturally would, all the particulate measurements are taken after the exhaust passes through a dilution tunnel. The dilution tunnel mixes the exhaust with clean ambient air and includes a residence chamber that allows the particles to age.

A heated sample line, set at 150°C, delivers the exhaust sample to the dilution tunnel and prevents the gases from condensing. A Venturi flow meter, also heated to 150°C, is used to measure the flow rate of sample exhaust air entering the dilution tunnel by relating the pressure drop across an orifice to volumetric flow. The dilution air is first cleaned by a HEPA filter, followed by an activated charcoal filter to en-

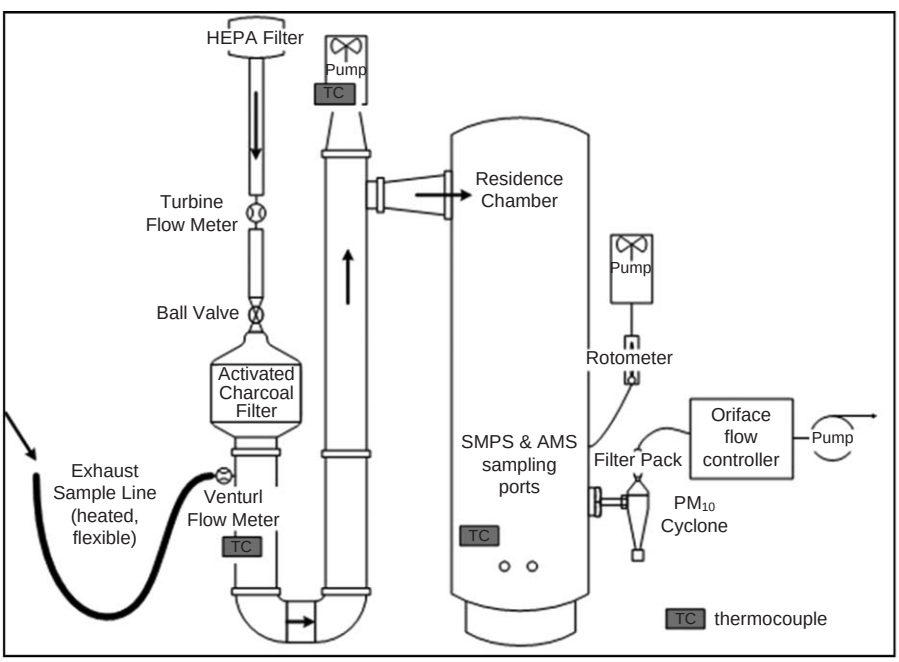

Fig. 1. Schematic diagram of dilution tunnel (adapted from Bennett *et al*., 2008).

sure that the dilution air is free of particles that may be present in the ambient air. A turbine flow meter is used to measure the flow rate of clean dilution air (dilution ratio of 40 : 1) (Fig. 1).

For the present study, at the higher loads, the turbocharger produces a higher pressure resulting in increased sample flow rate thereby decreasing the dilution ratio. To keep the dilution ratio constant at 40 : 1 for both engine loads (50% and 75%), the ball valve was closed slightly at the lower load. A pump was used to discharge air and exhaust from the residence chamber to control the residence time in the tunnel. For tests reported in this thesis, a valve and rotameter combination were set to allow 200 scfm (standard cubic feet per minute) of air and exhaust out of the tunnel. All of the particulate measurements were taken from the bottom of the residence chamber so that the dilution and aging of the particles would be complete before sampling. In this study, 5 minute time resolution will be used for determining non-refractory fine particle composition, including concentrations of nitrate, sulfate, and organic carbon.

3. RESULTS AND DISCUSSION

The AMS provides detailed information about the chemical composition of the particulate matter, with the exception of the elemental carbon. The volatile and semi-volatile particulates are ionized and fragmented before entering the mass spectrometer and the pieces of the original molecules are identified based on their mass-to-charge ratios. The results can be broken down in varying degrees of precision. All of the ions measured for each fuel can be broken down into organic and inorganic components. The inorganic content can be divided into sulfate, nitrate, and ammonium. Each of these categories can be segregated further into the individual molecule fragments. The AMS is also capable of measuring the particulate size distribution but the range of sizes detectable by the AMS, from 40 nm to 1 μm. Figs. 2 and 3 show the AMS results, divided into organic and inorganic particles depends on loading percent. Fig. 3 shows the breakdown of inorganic content between nitrate, sulfate and ammonium depends on loading percent.

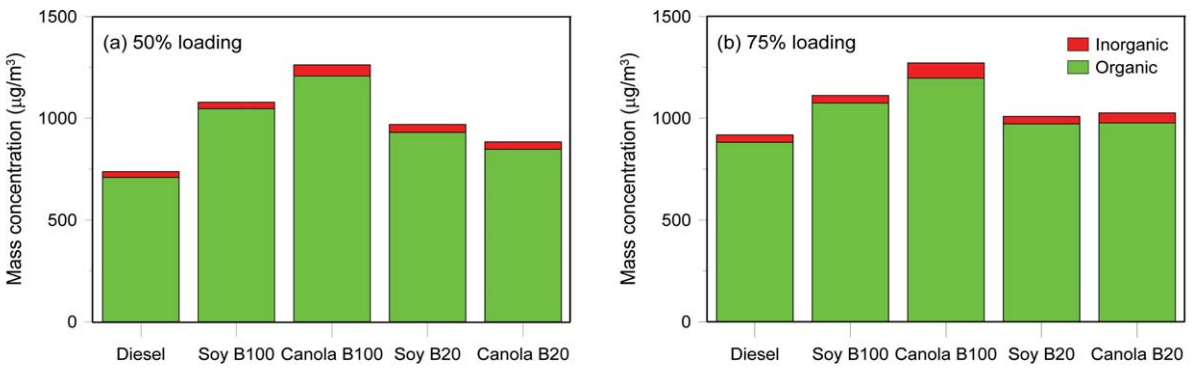

Fig. 2. Concentrations of organic carbon and inorganic for each fuel at (a) 50% load and (b) 75% load.

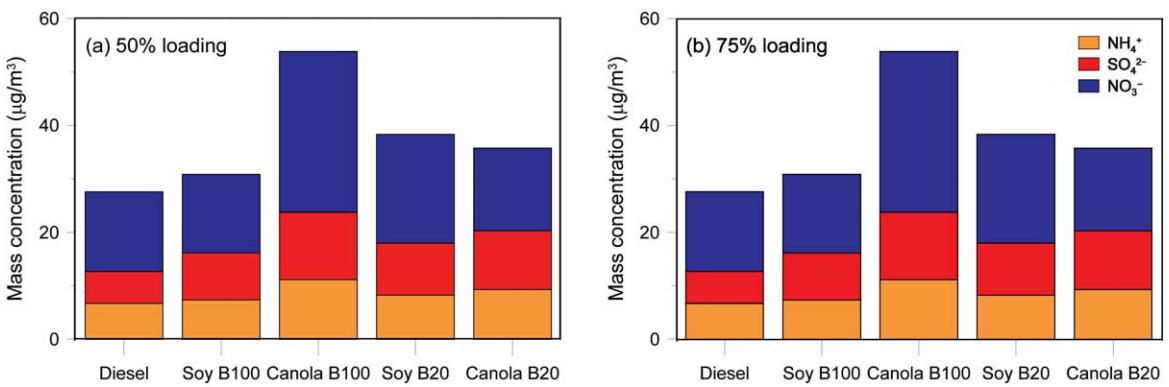

Fig. 3. Concentrations of inorganic aerosol components (ammonium, sulfate, and nitrate) at (a) 50% load and (b) 75% load.

At 50% load, the concentration of total mass emission ranged from ~750 to ~1250 μg/m^3 (Fig. 2(a)). Ultra-low sulfur diesel (ULSD) produces the least organics, followed by the Canola and Soy 20% blends. Of the 100% blends, Soy 100% blend produces the lowest amount of organics, while Canola 100% blend is the highest organics producers of the 100% blends. Similar trends are seen at the higher load (75% load) as shown in Fig. 2(b). Relative to the organic carbon content of the exhaust, the inorganic species make up a relatively small fraction of the volatile and semi-volatile exhaust products. For both 50% and 75% loads, ULSD and Soy B100 were the lowest producers of inorganic species, 3.8% (3.9% for 75% load) and 2.9% (3.3% for 75% load), respectively, and Canola B100 is the highest (4.4% and 5.8% for 50% and 75% loads, respectively) (not shown in this paper). Nitrate was generally the most abundant component in inorganic aerosol and ranged from 14.6 to 30.2 μg/m^3 as shown in Fig. 3. The nitrates produced by Canola 100% blend are significantly higher than for the other fuels for both 50% and 75% loads, making it the largest source for total inorganic species (more than 50% of total inorganic aerosol).

A main advantage of the HR-ToF-AMS data is the separate quantification of different ions with the same nominal mass, enabling precise characterization of the elemental composition of each ion (e.g. $C_xH_y^+$, $C_xH_yO_1^+$, and $C_xH_yO_z^+$). This enhanced information is useful for understanding the overall chemical characteristics of ambient organic aerosols and their evolution in the atmosphere. Fig. 4 depicts the contribution of three ion categories ($C_xH_y^+$, $C_xH_yO_1^+$, and $C_xH_yO_z^+$) of interest in organic aerosol (OA). Relative abundances of these fragments help describe the overall degree of OA oxidation. On average, the oxidized fragment families ($C_xH_yO_1^+$, and $C_xH_yO_z^+$) accounts for ~13% of the three family sum, while ~87% comes from the $C_xH_y^+$ family. It should be noted that the increase of $C_xH_yO_1^+$, and $C_xH_yO_z^+$ families is often associated with a decrease of the $C_xH_y^+$ family. This is important implications that OA mass is potentially increased a transformation processes from $C_xH_y^+$ family to $C_xH_yO_z^+$ family by oxidation in ambient.

Looking at individual molecular fragments from as identified by the AMS can identify content in the exhaust that differs significantly between ULSD and the biodiesel blends. Fig. 5 shows typical mass spectrum of ULSD and biodiesel obtained AMS. One such molecular fragment, as identified by the mass to charge ratio, is shown below in Fig. 6. Specifically, the two peaks of $C_2H_3O_2$ (*m/z* 59.01) and C_3H_7O (*m/z* 59.04) located at approximately *m/z* 59 are notable because the diesel exhaust (as signified by the red line in Fig. 6) produces significantly less of this molecular fragment in comparison with all of the methyl esters. This result has the potential to be of use for atmospheric scientists as a way of uniquely identifying the source of atmospheric particulate matter. Specifically, if diesel particulate matter contains little or no oxygenated hydrocarbon molecular fragments at 59.01 (Fig.

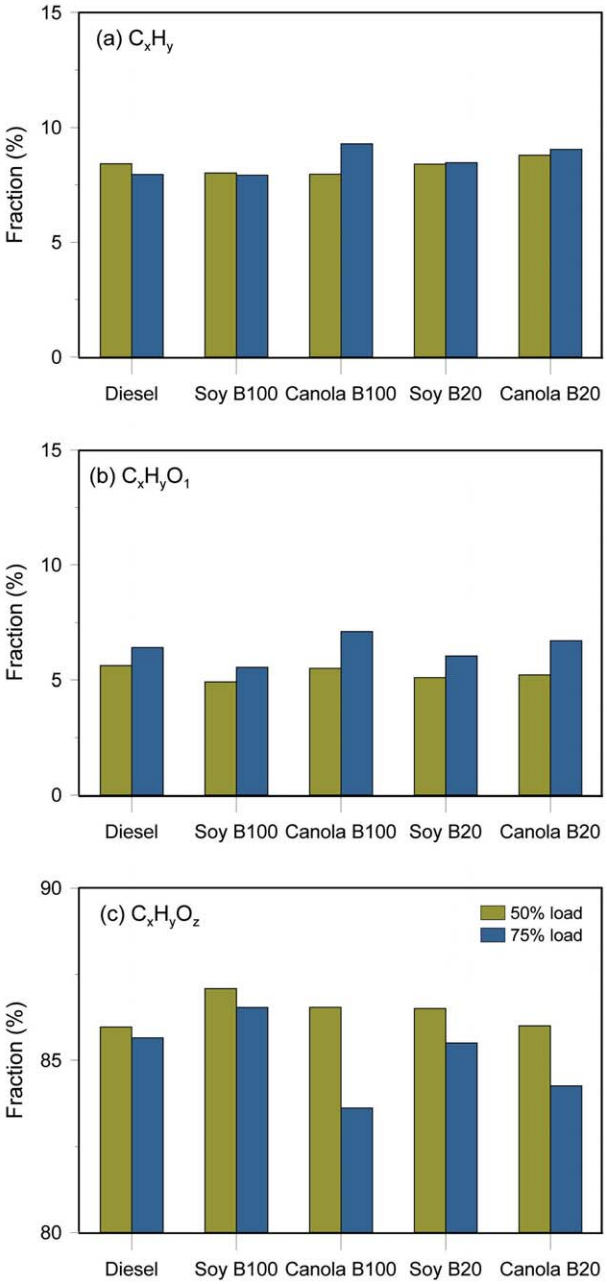

Fig. 4. Contributions of organic aerosol components to three ion categories depends on load ((a) C_xH_y, (b) C_xH_yO, (c) $C_xH_yO_z$).

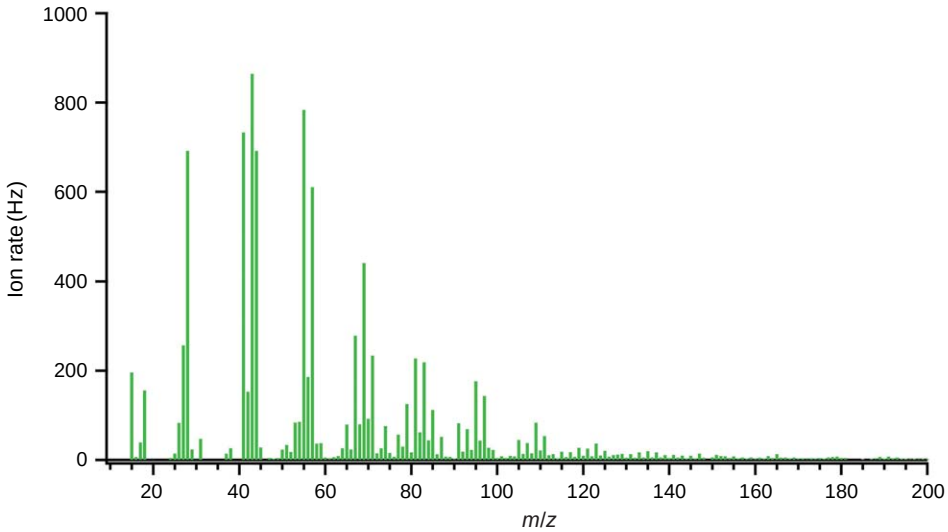

Fig. 5. Typical mass spectrum of biodiesel obtained by AMS.

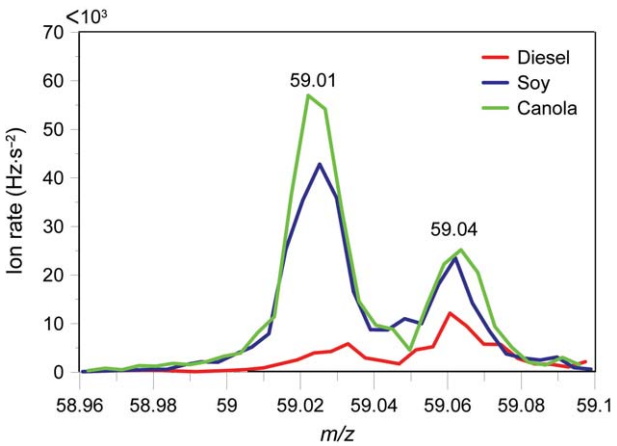

Fig. 6. Double spike for mass-to-charge ratio of 59 for 20% blends at 75% load.

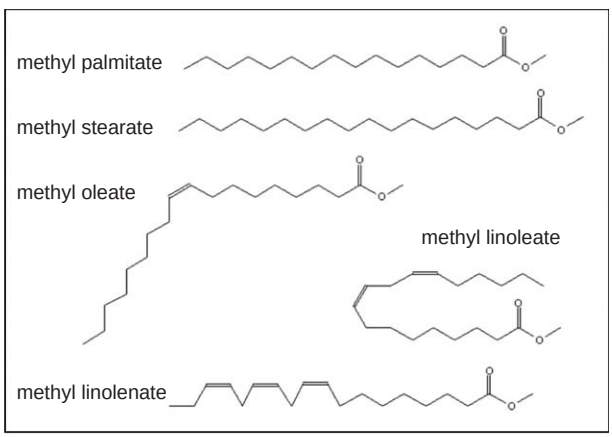

Fig. 7. Examples of the molecular structure of methyl esters.

6), then it may be possible to distinguish primary atmospheric diesel particulate matter from other sources such as biomass burning, or secondary organic aerosols. Part of the difficulty of using the AMS is taking a precise mass-to-charge ratio and making an educated guess as to what combination of atoms result in that mass. One likely combination that could produce the exact mass of these peaks is $C_2H_3O_2$ (59.01). All methyl ester molecules have a $C(=O)OCH_3$ group at one end (Fig. 7), so it is reasonable to expect that if any unburned fuel is present in the particulate matter in methyl ester exhaust that this fragment would be present in the AMS data.

The set of curves shown in Fig. 6 is a compilation of results from ULSD and the 20% biodiesel blends at 75% load. The other blends and loads show similar results. As mentioned above, these peaks could be used to identify atmospheric particulate matter directly to biodiesel exhaust, as distinguished from that created by petroleum diesel. Recent results suggest, however, that other types of biomass burning also produce the $C_2H_3O_2$ fragment (Lee *et al.*, 2010). However, the fact that petroleum diesel combustion does not produce this peak may still be a useful result.

4. CONCLUSIONS

Organics and nitrate were the dominant species in PM_1 with smaller contributions from ammonium and sulfate. Similar trends of chemical composition of

PM_1 are observed in both 50% and 75% loads of engine. Specific finding are detailed below.

- ULSD (ultra-low sulfur diesel) produces the lowest organic aerosols compared to the biodiesel. The concentration of organics on aerosols from Canola 100% was higher than that from Soy 100%.
- Inorganic species from ULSD and Soy B100 were the lowest concentration, but Canola B100 was remarkably the highest at both 50% and 75% loads, especially nitrate which is 2 times higher than ULSD.
- $C_xH_y^+$ family occupied dominant portion (~87%) among the fragment family, and the rest portion was shared with oxidized fragment families (~8% for $C_xH_yO_1^+$ and ~5% for $C_xH_yO_z^+$). It is important results from mass perspective that OA mass is potentially increased a transformation processes from $C_xH_y^+$ family to $C_xH_yO_z^+$ family by oxidation in ambient.
- The ratio of two peaks of $C_2H_3O_2$ (*m/z* 59.01) and C_3H_7O (*m/z* 59.04) located at approximately *m/z* 59 are notable between diesel and biodiesel. This result has the potential to be of use for atmospheric scientists as a way of uniquely identifying the source of atmospheric particulate matter.

ACKNOWLEDGEMENT

Data analysis and additional data processing were supported by Hankuk University of Foreign Studies Research Fund of 20141077001.

REFERENCES

Aakko, P., Nylund, N.O., Westerholm, M., Marjamaki, M., Moisio, M., Hillamo, R. (2002) Emissions from heavy-duty engine with and without aftertreatment using selected biofuels. In: FISITA 2002 world automotive congress proceedings, F02E195.

Appenzeller, T. (2004) The End of Cheap Oil. National Geographic, June 2004.

Bagley, S.T., Gratz, L.D., Johnson, J.H., McDonald, J.F. (1998) Effects of an Oxidation Catalytic Converter and a Biodiesel Fuel on the Chemical, Mutagenic, and Particle Size Characteristics of Emissions from a Diesel Engine. Environmental Science & Technology 32, 1183-1191.

Bennett, M., Volckens, J., Stanglmaier, R., McNichol, A.P., Ellenson, W.D., Lewis, C.W. (2008) Biodiesel effects on particulate radiocarbon (14C) emissions from a diesel engine. Journal of Aerosol Science 39, 667-678.

Chapman, L. (2007) Transport and climate change: a review. Journal of Transport Geography 15, 354-367.

Chirico, R., Clairotte, M., Adam, T.W., Giechaskiel, B., Heringa, M.F., Elsasser, M., Martini, G., Manfredi, U., Streibel, T., Sklorz, M., Zimmermann, R., DeCarlo, P.F., Astorga, C., Baltensperger, U., Prevot, A.S.H. (2014) Emissions of organic aerosol mass, black carbon, particle number, and regulated and unregulated gases from scooters and light and heavy duty vehicles with different fuels. Atmospheric Chemistry and Physics Discussion 14, 16591-16639.

DeCarlo, P.F., Kimmel, J.R., Trimborn, A., Northway, M.J., Jayne, J.T., Aiken, A.C., Gonin, M., Fuhrer, K., Horvath, T., Docherty, K.S., Worsnop, D.R., Jimenez, J.L. (2006) Field-Deployable, High-Resolution, Time-of-Flight Aerosol Mass Spectrometer. Analytical Chemistry 78, 8281-8289.

De Filippo, A., Maricq, M.M. (2008) Diesel nucleation mode particles: semivolatile or solid? Environmental Science and Technology 42, 7957-7962.

Demirbas, A. (2007) Importance of biodiesel as transportation fuel. Energy Policy 35, 4661-4670.

Di, Y., Cheung, C.S., Huang, Z. (2009) Comparison of the effect of biodiesel-diesel and ethanoldiesel on the particulate emissions of a direct injection diesel engine. Aerosol Sciecnce & Technology 43, 455-465.

Drewnick, F., Hings, S.S., DeCarlo, P., Jayne, J.T., Gonin, M., Fuhrer, K., Weimer, S., Jimenez, J.L., Demerjian, K.L., Borrmann, S., Worsnop, D.R. (2005) A New Time-of-Flight Aerosol Mass Spectrometer (TOF-AMS) - Instrument Description and First Field Deployment. Aerosol Science and Technology 39, 637-658.

Dutcher, D.D., Pagels, J., Bika, A., Franklin, L., Stolzenburg, M., Thompson, S., Medrano, J., Brown, N., Gross, D.S., Kittelson, D., McMurry, P.H. (2011) Emissions from soy biodiesel blends: A single particle perspective. Atmospheric Environment 45, 3406-3413.

Gaffney, J.S., Marley, N.A. (2009) The impacts of combustion emissions on air quality and climate - From coal to biofuels and beyond. Atmospheric Environment 43, 23-36.

Gordon, T.D., Presto, A.A., Nguyen, N.T., Robertson, W.H., Na, K., Sahay, K.N., Zhang, M., Maddox, C., Rieger, P., Chattopadhyay, S., Maldonado, H., Maricq, M.M., Robinson, A.L. (2014) Secondary organic aerosol production from diesel vehicle exhaust: impact of aftertreatment, fuel chemistry and driving cycle. Atmospheic Chemistry and Physics 14, 4643-4659.

Heikkilä, J., Virtanen, A., Rönkkö, T., Keskinen, J., Aakko-Saksa, P., Murtonen, T. (2009) Nanoparticle emissions from a heavy-duty engine running on alternative diesel fuels. Environmental Science & Technology 43, 9501-9506.

Jayne, J.T., Leard, D.C., Zhang, X., Davidovits, P., Smith, K.A., Kolb, C.E., Worsnop, D.R. (2000) Development of an Aerosol Mass Spectrometer for Size and Composition Analysis of Submicron Particles. Aerosol Science and Technology 33, 49-70.

Jimenez, J.L., Jayne, J.T., Shi, Q., Kolb, C.E., Worsnop, D.R., Yourshaw, I., Seinfeld, J.H., Flagan, R.C., Zhang, X., Smith, K.A., Morris, J.W., Davidovits, P. (2003) Ambient aerosol sampling using the Aerodyne Aerosol Mass Spectrometer. Journal of Geophysical Research: Atmospheres 108, 8425.

Karavalakis, G., Stournas, S., Fontaras, G., Samaras, Z., Dedes, G., Bakeas, E. (2009) The Effect of Biodiesel on PAHs, Nitro-PAHs and Oxy-PAHs Emissions from a Light Vehicle Operated Over the European and the Artemis Driving Cycles. SAE Technical Paper 2009-01-1895.

Kittelson, D.B. (1998) Engines and nanoparticles: a review. Journal of Aerosol Science 29, 575-588.

Kittelson, D.B., Watts, W.F., Johnson, J.P. (2006) On-road and laboratory evaluation of combustion aerosols part 1: summary of diesel engine results. Journal of Aerosol Science 37, 913-930.

Lapuerta, M., Armas, O., Rodríguez-Fernández, J. (2008) Effect of biodiesel fuels on diesel engine emissions. Progress in Energy and Combustion Science 34, 198-223.

Lee, T., Sullivan, A.P., Mack, L., Jimenez, J.L., Kreidenweis, S.M., Onasch, T.B., Worsnop, D.R., Malm, W., Wold, C.E., Hao, W.M., Collett, J.L. (2010) Chemical Smoke Marker Emissions During Flaming and Smoldering Phases of Laboratory Open Burning of Wildland Fuels. Aerosol Science & Technology 44, i-v.

Mayer, A., Czerwinski, J., Wyser, M., Mattrel, P., Heitzer, A. (2005) Impact of RME/Diesel Blends 5 on Particle Formation, Particle Filtration and PAH Emissions. SAE Technical Paper 2005-01-1728, doi:10.4271/2005-01-1728.

Middlebrook, A.M., Bahreini, R., Jimenez, J.L., Canagaratna, M.R. (2011) Evaluation of Composition-Dependent Collection Efficiencies for the Aerodyne Aerosol Mass Spectrometer using Field Data. Aerosol Science & Technology 46, 258-271.

National Biodiesel Board (2009) U.S. Biodiesel Production Capacity. U.S. Biodiesel Board.

Sheehan, J., Camobreco, V., Duffield, J., Graboski, M., Shapouri, H. (1998) An Overview of Biodiesel and Petroleum Diesel Life Cycles. NREL/TP-580-24772, NREL.

U.S. Department of Energy (2009) National Algal Biofuels Technology Roadmap. DOE Biomass Program, September 2014.

USEPA (United States Environmental Protection Agency) (2002) A Comprehensive Analysis of Biodiesel Impacts on Exhaust Emissions. EPA 420-P-02-001, October, 2014.

Young, L.-H., Liou, Y.-J., Cheng, M.-T., Lu, J.-H., Yang, H.-H., Tsai, Y.I., Wang, L.-C., Chen, C.-B., and Lai, J.-S. (2012) Effects of biodiesel, engine load and diesel particulate filter on nonvolatile particle number size distributions in heavy-duty diesel engine exhaust. Journal of Hazardous Materials 199-200, 282-289.

Zhu, L., Cheung, C.S., Zhang, W.G., Huang, Z. (2010) Influence of methanol-biodiesel blends on the particulate emissions of a direct injection diesel engine. Aerosol Science & Technology 44, 362-369.

(Received 13 February 2015, revised 17 February 2015, accepted 24 February 2015)